Cell

Adenovirus Serotype 5 Hexon Mediates Liver Gene Transfer

Simon N. Waddington,[1,13] John H. McVey,[2,13] David Bhella,[3] Alan L. Parker,[4] Kristeen Barker,[4] Hideko Atoda,[5] Rebecca Pink,[3] Suzanne M.K. Buckley,[1] Jenny A. Greig,[4] Laura Denby,[4] Jerome Custers,[6] Takashi Morita,[5] Ivo M.B. Francischetti,[7] Robson Q. Monteiro,[8] Dan H. Barouch,[9] Nico van Rooijen,[10] Claudio Napoli,[11,12] Menzo J.E. Havenga,[6] Stuart A. Nicklin,[4] and Andrew H. Baker[4,*]

[1]Department of Haematology, Haemophilia Centre and Haemostasis Unit, Royal Free and University College Medical School, London NW3 2PF, UK

[2]Haemostasis and Thrombosis, MRC Clinical Sciences Centre, Imperial College London, Du Cane Road, London W12 0NN, UK

[3]Medical Research Council Virology Unit, University of Glasgow, Church Street, Glasgow G11 5JR

[4]British Heart Foundation Glasgow Cardiovascular Research Centre, University of Glasgow, 126 University Place, Glasgow G12 8TA, UK

[5]Department of Biochemistry, Meiji Pharmaceutical University, 2-522-1, Noshio, Kiyose, Tokyo, Japan

[6]Crucell, PO Box 2048, 2301 CA Leiden, The Netherlands

[7]Laboratory of Malaria and Vector Research, NIAID/NIH, Rockville, MD 20892-8132, USA

[8]Instituto de Bioquimica Medica, Universidade Federal do Rio de Janeiro, Brazil

[9]Division of Viral Pathogenesis, Beth Israel Deaconess Medical Center, Harvard Medical School, Boston, MA 02215, USA

[10]Department of Molecular Cell Biology, Vrije Universiteit, VUMC, 1081 BT Amsterdam, The Netherlands

[11]Department of General Pathology, II University of Naples, Naples 80138, Italy

[12]Sbarro Institute for Cancer Research and Molecular Medicine, College of Science and Technology, Temple University, Philadelphia, PA 19122, USA

[13]These authors contributed equally to this work.

*Correspondence: ab11f@clinmed.gla.ac.uk

DOI 10.1016/j.cell.2008.01.016

SUMMARY

Adenoviruses are used extensively as gene transfer agents, both experimentally and clinically. However, targeting of liver cells by adenoviruses compromises their potential efficacy. In cell culture, the adenovirus serotype 5 fiber protein engages the coxsackievirus and adenovirus receptor (CAR) to bind cells. Paradoxically, following intravascular delivery, CAR is not used for liver transduction, implicating alternate pathways. Recently, we demonstrated that coagulation factor (F)X directly binds adenovirus leading to liver infection. Here, we show that FX binds to the Ad5 hexon, not fiber, via an interaction between the FX Gla domain and hypervariable regions of the hexon surface. Binding occurs in multiple human adenovirus serotypes. Liver infection by the FX-Ad5 complex is mediated through a heparin-binding exosite in the FX serine protease domain. This study reveals an unanticipated function for hexon in mediating liver gene transfer in vivo.

INTRODUCTION

Adenoviruses are common pathogens used experimentally and in completed and ongoing clinical trials for gene delivery in oncology, cardioangiology, and regenerative medicine and as vaccine vectors (Schenk-Braat et al., 2007; Kawabata et al., 2006). Much work has demonstrated the potential benefits and limitations of adenovirus-mediated gene therapy preclinically and clinically, the latter being brought to the forefront by the death of Jesse Gelsinger in 1999 in response to very high-dose adenovirus type 5 (Ad5) delivered directly into the hepatic artery (Raper et al., 2003). This dramatically highlighted the need to fully understand the virological and biological aspects that define adenovirus infectivity of liver and toxicity in vivo before vectors could be fully optimized for clinical use.

Adenoviruses based on human serotype 5 have been studied extensively, yet fundamental issues relating to infection mechanisms remain to be elucidated, particularly in vivo. Adenoviruses are principally made up of three major capsid proteins—hexon, penton, and fiber. The crystal structures of Ad2 and Ad5 hexon have been solved (Athappilly et al., 1995; Roberts et al., 1986; Rux and Burnett, 2000) and reveal a complex structure. The hexon, the major site of antigenicity in adenoviruses (Pichla-Gollon et al., 2007; Roberts et al., 2006; Sumida et al., 2005), is the most abundant capsid protein and is positioned at the virion surface, arranged into 240 homotrimeric structures interlinked from neighboring monomers, thus providing structural support. The fiber which engages the penton base at the capsid surface projects away from the virion (San Martin and Burnett, 2003), is highly variable in length, and is thought to be the major site determining cell infectivity (reviewed in Nicklin et al., 2005). For subgroup C adenoviruses, including Ad5, the globular fiber knob positioned at the end of the trimeric fiber shaft binds the coxsackievirus and adenovirus receptor (CAR), expressed in an anatomically similar manner in mice and humans (Bergelson et al., 1997; Tomko et al., 1997), whereas subgroup B adenoviruses

utilize CD46, which is ubiquitously expressed in humans but limited to the testes in mice (Gaggar et al., 2003; Segerman et al., 2003). Ad5 internalization is mediated by integrin engagement with the penton base (Wickham et al., 1993). Extensive research efforts have primarily focused on the fiber protein for analysis of cell interactions in diverse gene therapy applications.

Following intravascular delivery, an important route of administration for many clinical applications, liver is the predominant site of Ad5 sequestration with substantial hepatocyte transduction (Huard et al., 1995). Ad5 vectors engineered through mutagenesis to lack CAR binding show identical liver transduction following intravascular injection in rodents and nonhuman primates (Alemany and Curiel, 2001; Smith et al., 2003) indicating alternate route(s) to gene transfer in vivo. A number of plasma proteins, including coagulation factor IX (FIX) and complement binding protein-4 (C4BP) were shown, using an ex vivo perfusion model, to bind the Ad fiber knob and "bridge" the virus to alternate receptors in liver, thus potentially bypassing CAR (Shayakhmetov et al., 2005). We showed using surface plasmon resonance (SPR) that Ad5 bound directly to the vitamin K-dependent coagulation factor X (FX) (Parker et al., 2006). In mice pretreated with warfarin (to ablate functional levels of vitamin K-dependent coagulation factors) liver infection was reduced by several orders of magnitude for both CAR-binding and CAR-binding-mutant Ad5 vectors (Parker et al., 2006; Waddington et al., 2007), suggesting an important function for host factors in liver targeting. Injection of physiological levels of FX into warfarin-treated mice prior to intravenous Ad5 injection fully restored liver gene transfer (Parker et al., 2006; Waddington et al., 2007).

Based on this, Ad5, and potentially other adenoviruses, engage host proteins for liver infection. Here, we characterize FX-Ad5 binding in detail and reveal binding of FX to the Ad5 hexon, not fiber. Binding occurs between the hexon hypervariable regions (HVRs) and the FX Gla domain with cell binding dictated by the FX serine protease domain. Thus, we provide evidence for an unexpected function of the Ad5 hexon protein in cell infectivity through recruitment of host FX. We also show that this interaction extends to other (but not all) human adenovirus species from multiple subgroups, indicating that it arose early in the evolution of adenovirus as a pathogen.

RESULTS

The FX Gla Domain Is Required for Ad5 Binding

FX is a zymogen of a vitamin K-dependent serine protease with a Gla (γ-carboxylated glutamic acid)-EGF1 (epidermal growth factor-like)-EGF2-SP (serine protease) domain structure (Figure 1A) that circulates in plasma at a concentration of 8 μg/ml. FX is converted to its active serine protease by a single proteolytic cleavage generating a two-chain disulphide-linked molecule consisting of a light chain (LC; Gla-EGF1-EGF2) and a heavy chain (HC; SP). There are three calcium ion binding sites in the FX molecule—the Gla domain co-ordinates seven calcium ions, and EGF1 and the SP domain each bind a single calcium ion. The FX-Ad5 interaction is calcium dependent (Parker et al., 2006). We sought to identify the domain responsible for Ad5 binding. To ascertain whether the N-terminal Gla-EGF1 component of FX bound Ad5 we assessed binding to full-length activated human FX (FXa; Gla-EGF1-EGF2-SP) and a human FXa mutant containing the C-terminal EGF2-SP domain (EGF2-SP FXa). The EGF2-SP fragment failed to bind Ad5, which however did show efficient binding to full-length FXa (Figure 1B). This suggests an absolute requirement for Gla-EGF1 in Ad5 binding. This was confirmed using a monoclonal antibody (HX-1) directed to the LC of FX (Gla-EGF1-EGF2) that blocked the interaction of Ad5 with human FX (Figure 1C) and abolished human FX-mediated gene transfer in vitro (for in vitro studies we used the CAR binding-ablated virus, AdKO1[Parker et al., 2006], since the use of this virus mimics the CAR-independent liver gene transfer by Ad5 observed in vivo [Parker et al., 2006; Waddington et al., 2007]) (Figure 1D). To demonstrate the importance of the Gla domain in Ad5 binding we analyzed the interaction of Ad5 with Gla domainless human FX (FX-GD) by SPR. The effect of the FX Gla domain opposes our earlier report (Parker et al., 2006) where we showed that both FX and FX-GD evoked equivalent enhancements of in vitro cell transduction mediated by Ad5. The FX-GD utilized was subsequently shown to contain a significant quantity of full-length FX by western blot analysis. For the present study we therefore used FX-GD additionally purified by affinity chromatography using an anti-Gla antibody. Whereas Ad5 bound to full-length human FX in a concentration-dependent manner, Ad5 failed to bind human FX-GD (Figure 1E). In contrast HX-1 bound to both full-length FX and FX-GD (data not shown). We attempted to produce purified Gla domain alone by enzymatic digestion of FX but insufficient quantities for analysis were obtained. To confirm the importance of this interaction in vivo, we pretreated mice with warfarin to ablate circulating levels of functional vitamin K-dependent zymogens and showed that human FX-GD failed to rescue Ad5-mediated liver transduction (Figure 1F) despite achieving "normal" (8 μg/ml) physiological plasma concentrations of FX (98%) and FX-GD (106%) as measured by human FX-specific ELISA at 45 min post-infection with Ad5 (75 min post-injection of zymogen). Hence, the FX Gla domain is required for interaction with Ad5.

FX Binds to the Ad5 Hexon

To determine the FX-binding site on Ad5, we initially focused on the Ad5 fiber since it determines infectivity via CAR (Bergelson et al., 1997; Tomko et al., 1997). The interaction of Ad5 with FIX was identified through a knob-mediated interaction (Shayakhmetov et al., 2005). To evaluate FX binding to Ad5 fiber, we used a series of Ad5 vectors deleted of fiber knob alone, or fiber knob and sequential fiber shaft deletions (Ad5-21R and Ad5-7.5R; [Li et al., 2006), Figure 2A]), or a fully fiberless Ad5 particle (Ad5-ΔF; Von Seggern et al., 1999). Shaft mutants make use of a fiber shaft trimerization motif for stable trimer formation in the absence of knob (Li et al., 2006). All mutant adenoviruses bound human FX efficiently as determined by SPR (Figure 2B). We exposed cells to each adenovirus in the presence or absence of physiological levels of human FX and quantified cell binding. In each case the level of binding is low in the absence of FX but strongly enhanced in its presence, even for fiberless particles (Figure 2C). This suggests that FX binds an alternate Ad5 capsid protein. Although the hexon is thought to act principally as a structural capsid protein, based on its abundance and exposure at the virion surface we next used SPR to determine

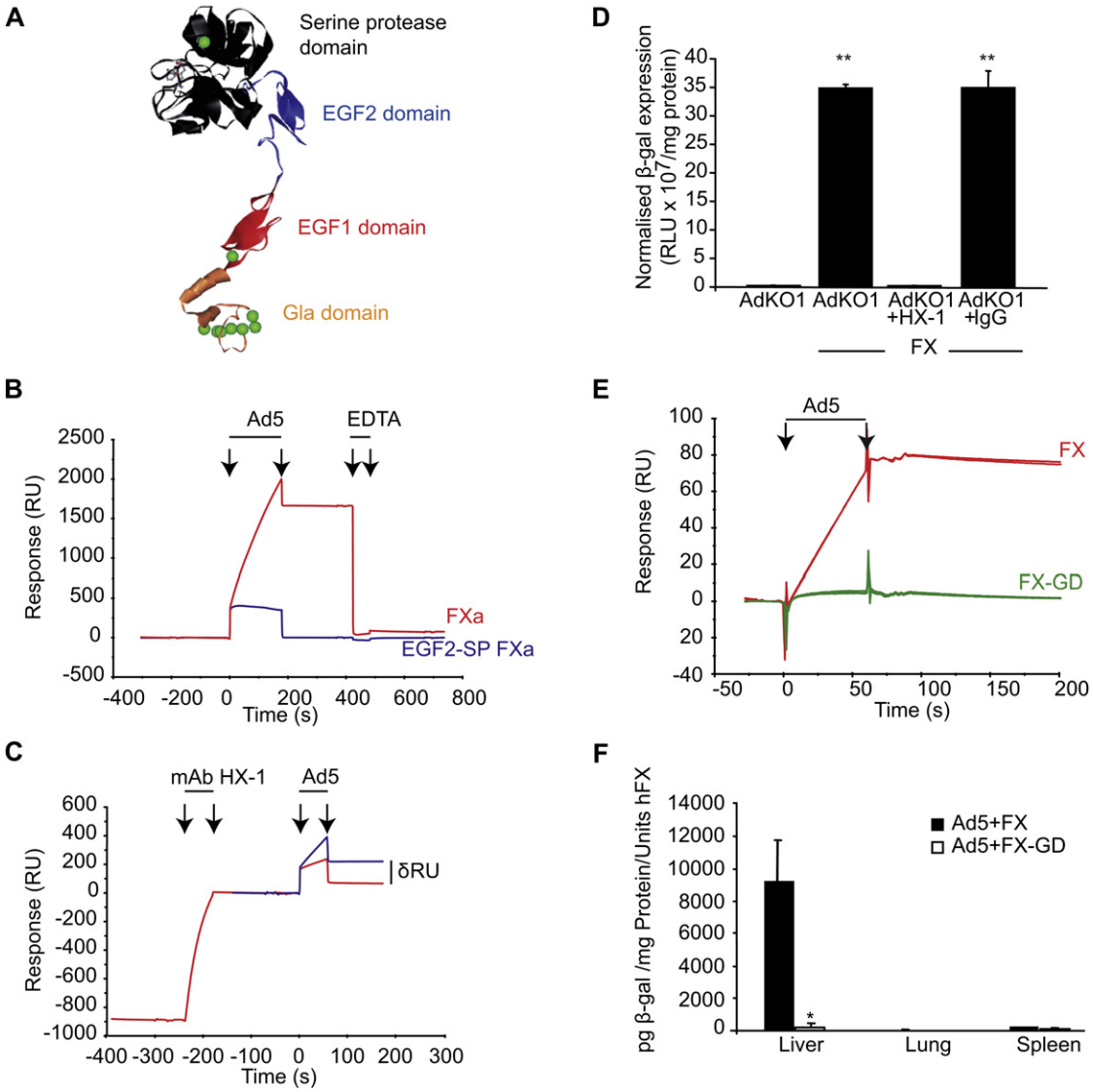

Figure 1. Analysis of FX Binding to Ad5

(A) Domain structure of human FX. Green balls indicate calcium ions.

(B) Coagulation factors (FXa, EGF2-SP FXa) were covalently coupled to SA biosensor chip. Depicted are overlayed sensorgrams. Arrows indicate the start and end of reagent injection. RU = response units.

(C) Antibody HX-1 directed against FX Gla-EGF1 was preinjected over the FX biocensor chip prior to Ad5 injection. HX-1 reduces FX-Ad5 binding (δRU). Arrows indicate the start and end of reagent injection.

(D) HepG2 cells were exposed to AdKO1 in the presence of physiological FX levels. FX was preincubated with antibody HX-1 or IgG isotype-matched control. Cell transduction was quantified at 72 hr post-infection (**$p < 0.001$ versus control). Errors bars represent SEM.

(E) SPR analysis of Ad5 binding to FX and FX-GD that lacks the FX Gla domain. A subtracted sensorgram (FXI used as control for nonspecific binding) is shown. Arrows indicate the start and end of reagent injection.

(F) MF-1 mice were pretreated with control peanut oil or warfarin and injected with 4×10^{11} VP/mouse Ad5 with or without preinjection of FX or FX-GD 30 min prior to virus injection. Quantitative ELISA for β-galactosidase shows levels in liver, spleen, and lung (*$p = 0.03$). Error bars represent SEM.

whether FX bound hexon. We observed a direct, calcium-dependent high-affinity interaction between purified Ad5 hexon and human FX (Figure 2D). The calculated association rate constant (ka) and dissociation rate constant (kd) values of the FX for immobilized hexon were 2.28×10^6 (1/Ms) and 4.5×10^{-3} (1/s) giving an overall equilibrium dissociation constant (K_D) of 1.95×10^{-9}M. When FX was immobilized and hexon was injected across the biosensor, calculated ka and kd values were 2×10^5 (1/Ms) and 4.1×10^{-3} (1/s) giving an overall K_D of 1.94×10^{-8}M. To assess the affinity of FX for the intact virus Ad5 was biotinylated and coupled to a streptavidin coated biosensor chip. The calculated ka and kd values were 1.2×10^6 (1/Ms) and 2.23×10^{-3} (1/s) giving an overall K_D of 1.83×10^{-9}M (Figure S1 available online).

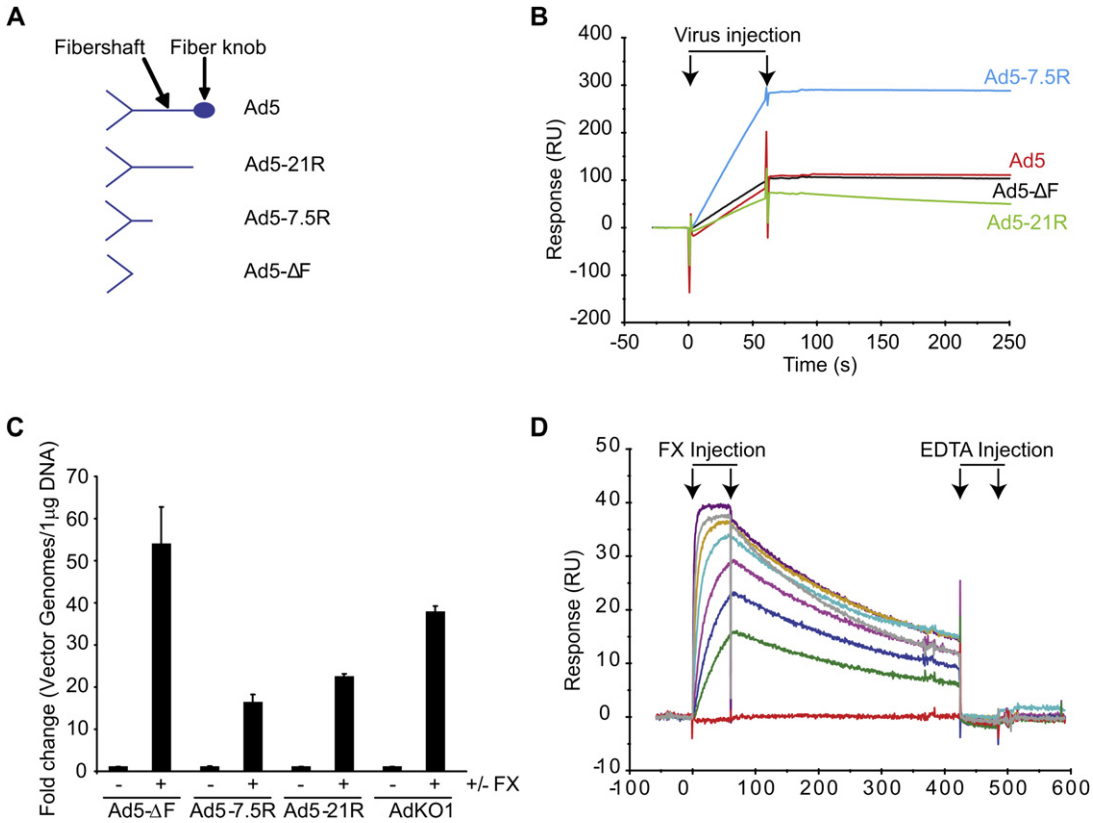

Figure 2. The Ad5 Hexon, Not Fiber, Binds to FX

(A) Representation of fiber mutants used to assess binding of FX to Ad5. Ad5-21R contains 21 shaft repeats but no knob, Ad5-7.5R contains just 7.5 shaft repeats, and Ad5-ΔF contains no fiber.

(B) Viruses were injected onto biosensor chips and binding to FX assessed. Subtracted sensorgrams (FX-FXI) are shown. Arrows indicate the start and end of reagent injection.

(C) HepG2 cells exposed to each adenovirus in the presence or absence of physiological FX levels. Cell-bound adenovirus was quantified. Error bars represent SEM.

(D) Purified Ad5 hexon protein was immobilized and binding to FX was analyzed. Sensorgrams are shown for injections at seven different concentrations of FX (50 to 0.781 μg/ml in a two-fold dilution series). The analysis was performed in triplicate. Injection of EDTA regenerated the biosensor chip surface. Arrows indicate the start and end of reagent injection.

Electron Cryomicroscopy and Three-Dimensional Reconstruction of Ad5 Bound to FX

To visualize the interaction between Ad5 and FX, three-dimensional (3D) reconstructions were calculated from cryomicrographs of both Ad5 and Ad5 complexed with FX. A total of 251 Ad5 and 305 FX-Ad5 virus particle images were used to compute reconstructions at 26 Å and 23 Å resolution, respectively (Figures 3A and 3B). These maps clearly reveal that the principal point of contact between Ad5 and FX occurs within the cup formed at the center of each hexon trimer (Figures 3C–3F), supporting the FX-hexon interaction seen by SPR. The structural information from the FX component that extends from the capsid surface is noisy and attenuated due to low occupancy (<50%) and incoherent averaging with FX components bound to adjacent hexons (Figure S2). The FX density at the binding site is significantly stronger and shows symmetry congruent with the hexon trimer. Such symmetry is not present in FX, suggesting that FX molecules bind to one of three potential binding sites in each hexon trimer, occluding the two remaining symmetry-related sites. FX density is then subject to three-fold averaging in the reconstruction. Modeling this interaction by fitting a high-resolution model of FX (Venkateswarlu et al., 2002) to our reconstructions strongly supports this interpretation (Figure S2). Moreover, SPR analysis indicates a stoichiometery of binding of 205 FX molecules per virus particle consistent with one FX molecule binding to each hexon trimer. Interestingly, the region containing the FX-binding site in hexon is characterized by the presence of HVRs (Rux and Burnett, 2000). We investigated this by SPR analysis of an Ad5 mutant in which all HVRs have been replaced by those from Ad48 (Ad5HVR48; [Roberts et al., 2006](Figure 4A)). The remainder of the capsid structure is entirely derived from Ad5. Ad48 did not bind FX (Figure 4B) and neither did the Ad5HVR48 mutant (Figure 4B). Next, we determined the effect of HVR replacement on infectivity. As Ad5HVR48 contains a wild-type Ad5 fiber without a CAR-binding mutation, we used human cells with low CAR levels (SKOV3 cells) for in vitro dissection of FX-mediated cell binding and transduction mediated by Ad5, Ad5HVR48, and Ad48. The HVR replacement resulted in a loss of FX-mediated

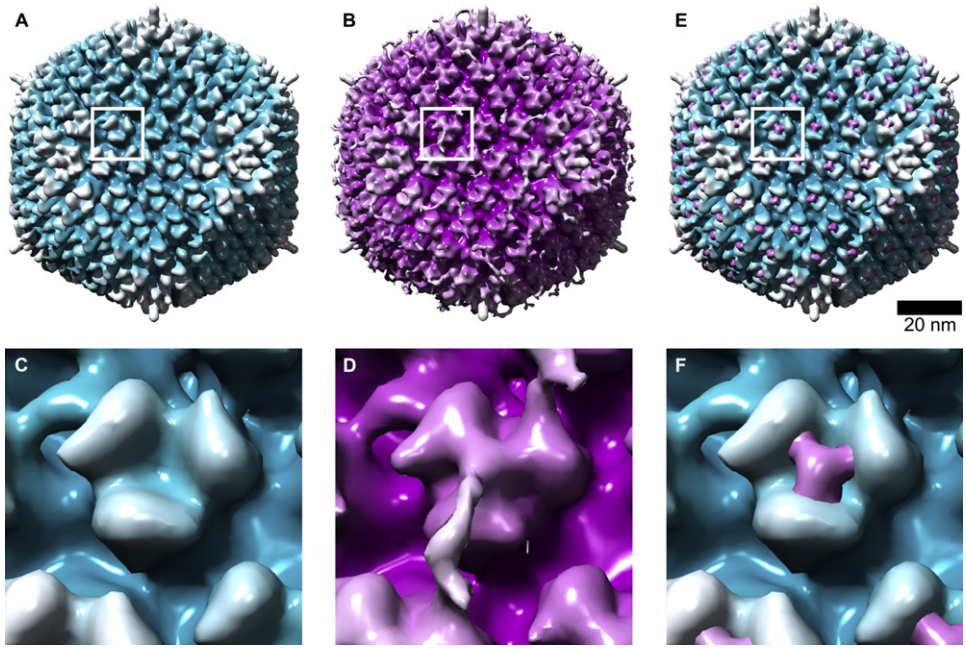

Figure 3. Analysis of Ad5 Hexon Binding to FX by Cryoelecton Microscopy

(A and B) Three-dimensional reconstructions of uncomplexed Ad5 (A) and FX-Ad5 complex (B) surface contoured to include density above the mean plus one standard deviation of total map density.

(C and D) Closeup view of an uncomplexed (C) and FX-complexed (D) hexon.

(E) Overlaid reconstructions of uncomplexed Ad5 (blue) and FX-Ad5 complex (purple). The scale bar represents 20 nm. The surface threshold level of the FX-Ad5 structure is raised to highlight the point of contact between FX and Ad5 hexon.

(F) Closeup view of FX-labeled hexon.

enhancement of cell binding (Figure 4C) and transduction (Figure 4D). An identical effect was obtained using the MDA-MB-435 cell line (Figure S3). We next assessed liver gene transfer in mice mediated by Ad5 and Ad5HVR48. Liver transduction, measured at 3 doses 48 hr post-intravascular injection demonstrated substantial reduction with Ad5HVR48 compared to Ad5 (Figure 4E). At the highest dose (5×10^{10} VP/mouse) an over 600-fold reduction in liver transgene expression was observed. This contrasted with direct intramuscular injection, where Ad5- and Ad5HVR48-driven transgene expression was not different (Figure 4E). Thus, replacement of the Ad5 hexon HVRs with those from Ad48 ablated FX binding, cell binding, and transduction in vitro and reduced liver transduction in vivo.

Liver Gene Transfer by the FX-Ad5 Complex

Blood coagulation proteases have evolved versatile and sensitive mechanisms for controlling the specificity of protein substrate recognition mediated by surface sites on the SP domain that are physically separate from the active site residues (exosites). The FX SP domain contains a heparin-binding exosite (exosite II) (Rezaie, 2000). We had previously shown that FX-enhanced transduction of cells required heparan sulfate proteoglycans (Parker et al., 2006, 2007) and therefore investigated a role for this exosite in transduction of the FX-Ad5 complex. We employed naturally occurring anticoagulants that bind FX exosite II: nematode anticoagulant peptide-2 (NAPc2), an 85 amino acid polypeptide that is a potent FX-dependent inhibitor and binds human FX with high affinity ($K_D = 7.28 \times 10^{-11}$M; Table S1; Figure 5A) (Murakami et al., 2007), and Ixolaris a 15.5 kDa two-Kunitz domain protein isolated from tick salivary gland that also binds human FX with high affinity ($K_D = 1.30 \times 10^{-9}$M; Table S1; Figure 5A) (Monteiro et al., 2005). SPR analysis revealed high-affinity interaction between either NAPc2 and FX or Ixolaris and human FX; however saturating amounts of either had no effect on Ad5 binding to human FX (Figure 5B). NAPc2 or Ixolaris eliminated the ability of FX to enhance Ad5 transduction in vitro, an effect observed at concentrations at or above the dissociation constant (K_D) for NAPc2-FX and Ixolaris-FX binding (Table S1; Figure 5C). This effect was due to reduced cell-surface binding of FX-Ad5 in the presence of inhibitor (Figure S4). In vivo, preincubation of FX with NAPc2 or Ixolaris prior to injection into warfarin-treated mice led to a substantial reduction in FX liver rescue (Figure 5D). Hence, binding of human FX to the Ad5 hexon through the Gla domain leads to cell transduction in vivo mediated through a heparin-binding exosite in the FX SP domain.

Pharmacological Blockade of Ad5 Hexon Binding to FX Blocks Gene Transfer In Vivo

The treatment of mice with warfarin offers the potential to study each vitamin K-dependent coagulation factor (FVII, FIX, FX, protein C) in isolation by complementation (Parker et al., 2006). Under such conditions, FX is the only coagulation factor capable of rescuing liver transduction mediated by Ad5 (Figure S5). The affinity of binding of each coagulation factor to purified Ad5 hexon

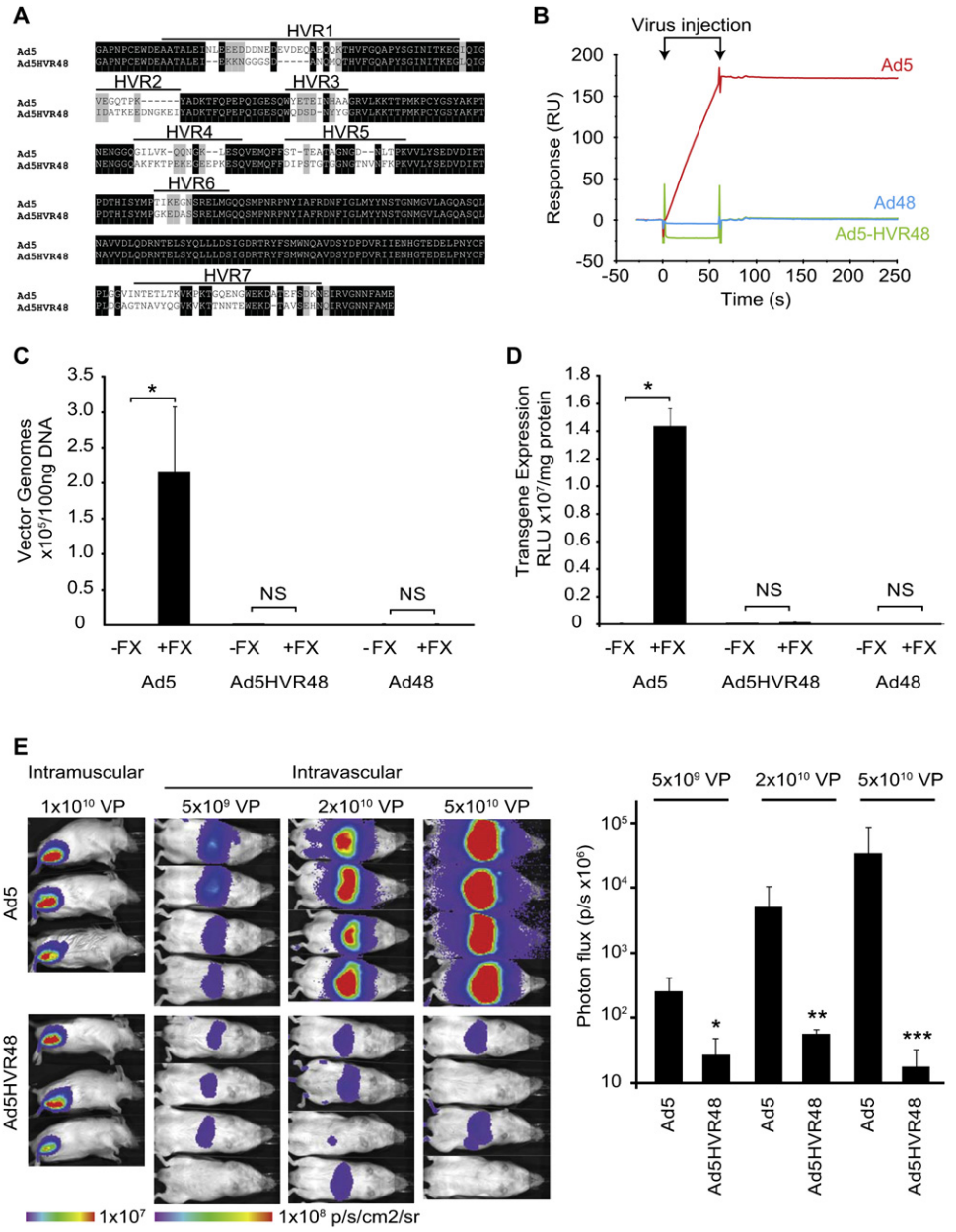

Figure 4. Analysis of FX Binding and Adenovirus Infection in an HVR-Modified Ad5 Vector

(A) Sequence alignment of amino acids of Ad hexon HVRs from Ad5 and the Ad5HVR48 mutant. White on black identical residues, black on gray similar residues, and black on white nonidentical residues. The HVRs (1–7) are indicated.

(B) Ad5 binding to FX is abolished by replacement of Ad5 HVRs with those from Ad48, analyzed by SPR (subtracted FX-FXI sensorgrams). Arrows indicate the start and end of reagent injection.

(C) SKOV3 cells were exposed to each adenovirus as indicated in the presence or absence of physiological FX levels for 1 hr at 4°C. DNA was extracted and cell-bound adenovirus quantified. Error bars represent SEM ($p < 0.05$ versus absence of FX).

(D) SKOV3 cells were exposed to each adenovirus as indicated in the presence or absence of physiological FX levels for 3 hr at 37°C. Transgene expression was quantified at 48 hr post-infection. Error bars represent SEM ($p < 0.05$ versus absence of FX).

(E) MF-1 mice were injected via the intravascular route with Ad5 or Ad5HVR48 at 5×10^9, 2×10^{10}, or 5×10^{10} or VP/mouse and luciferase imaged at 48 hr and quantified as photon flux. Intramuscular injections are shown as a comparison. Error bars represent SEM. *p = 0.00018, **p = 0.00002, ***p = 0.01368 versus Ad5.

was quantified by SPR (Figure S6), again showing differential kinetics for each coagulation factor and the predominant role for FX in this interaction. It is important to ascertain the global importance of the FX-Ad5 interaction in the presence of all other vitamin K-dependent zymogens under physiological conditions in vivo. This is essential for further understanding of the

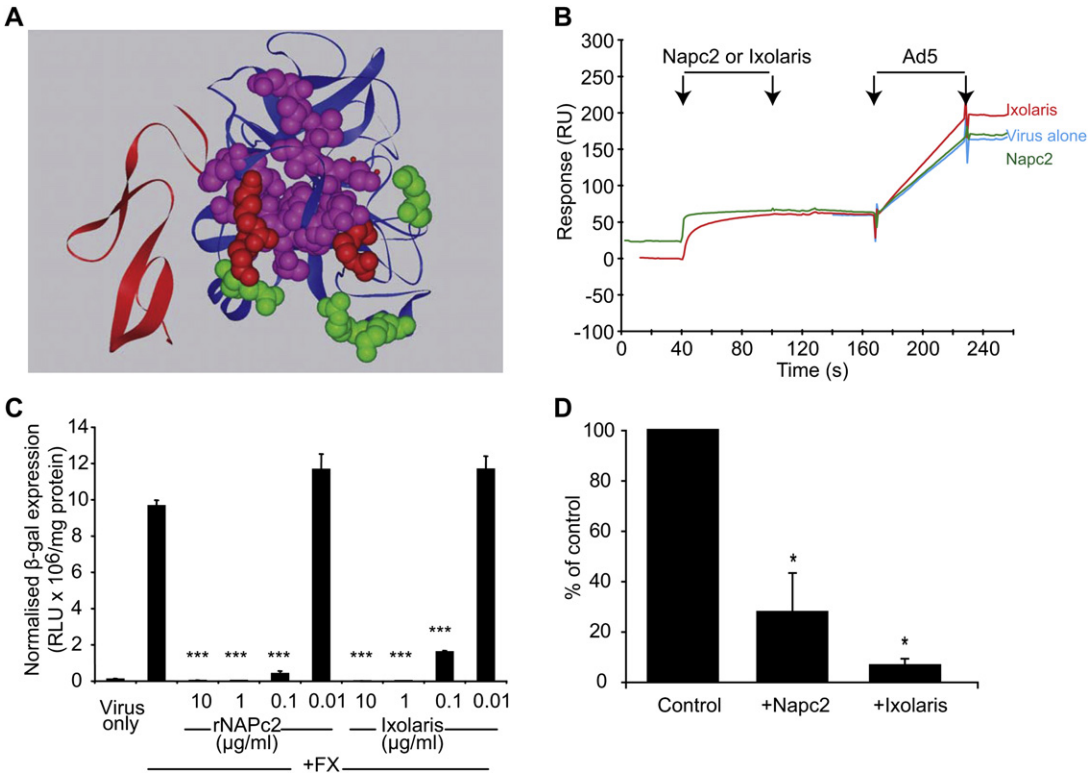

Figure 5. Gene Transfer of Liver by the FX-Ad5 Complex Is Mediated through an Exosite in FX

(A) Ribbon diagram of FX (EGF2-SP; PDB: 1HCG) to show NAPc2 (purple), Ixolaris (green), and overlapping (red) amino acid residues within their FX binding sites (Monteiro et al., 2005; Murakami et al., 2007).

(B) Subtracted SPR sensorgrams (FX-FXI) showing NAPc2 or Ixolaris binding to FX without inhibition of subsequent FX-Ad5 binding. Arrows indicate the start and end of reagent injection.

(C) HepG2 cells were exposed to AdKO1 in the presence or absence of physiological FX ± NAPc2 or Ixolaris at increasing concentrations. Transduction was quantified at 72 hr post-infection. Error bars represent SEM. ***$p < 0.01$ versus AdKO1 + FX.

(D) MF-1 mice were pretreated with control peanut oil or warfarin and injected with 4×10^{11} VP/mouse Ad5 with or without preinjection of FX alone or preincubated with three-fold molar excess of either NAPc2 or Ixolaris. Quantitative ELISA for β-galactosidase levels in liver was performed 48 hr later and compared to levels in the liver achieved by FX infusion alone. Error bars represent SEM. *$p < 0.05$ versus control.

importance of the interaction and how this may be used to design and implement inhibitors to block liver transduction by Ad5. X-bp is a 29 kDa protein, isolated from *Deinagkistrodon acutus* (the hundred pace snake), that binds with high affinity to the Gla domain of human and murine FX (Atoda et al., 1998) (Table S1). We thus utilized X-bp to define the effect of blockade of the FX-Gla domain-Ad5 interaction on cell transduction in vitro and in vivo. X-bp blocked the human FX-Ad5 interaction as evidenced by SPR, further demonstrating the importance of the Gla domain in FX binding to Ad5 (Figure 6A). In vitro, preincubation of human FX with X-bp at equimolar or higher concentrations prior to addition of Ad5 to cells abolished the FX-mediated enhancement in Ad5 transduction (Figure 6B). In vivo, X-bp when preincubated with FX prior to injection blocked the ability of human FX to rescue liver transduction by Ad5 in warfarinized mice (Figure 6C). Importantly, preinjection of wild-type control (non-warfarinised) mice with X-bp substantially reduced liver transduction mediated by a subsequent injection of Ad5 (Figure 6D). These findings were repeated in a second species (rat; Figure S7). Hence, based on our knowledge of the Ad5 hexon-FX interaction we have identified an efficient and simple pharmacological approach to block Ad5-mediated liver transduction following intravascular delivery.

FX Binding to Other Human Ad Serotypes

The human adenovirus family is substantial with over 50 serotypes, divided into subgroups A–F on the basis of hemagglutination, oncogenic properties, and DNA sequence identity. Many adenoviruses are being exploited for application to treat human diseases or for vaccination. A number of these approaches use adenoviruses derived entirely from alternate serotypes (Abbink et al., 2007; Lecollinet et al., 2006; Sakurai et al., 2006; Vogels et al., 2003), although many strategies simply use the Ad5 capsid but exchange the Ad5 fiber for the fiber from an alternate serotype (also called pseudotyping) (Gaggar et al., 2003; Shayakhmetov et al., 2000, 2002). Clearly, since FX binds the Ad5 hexon, the pseudotyping strategy will result in viruses that still possess FX-binding capacity and may possess FX-mediated infectivity effects in vitro and in vivo (Parker et al., 2007; Waddington et al., 2007). There are distinct advantages to using complete serotypes that have rare pre-existing immunity in the human population (Abbink et al., 2007; Vogels et al., 2003) for clinical

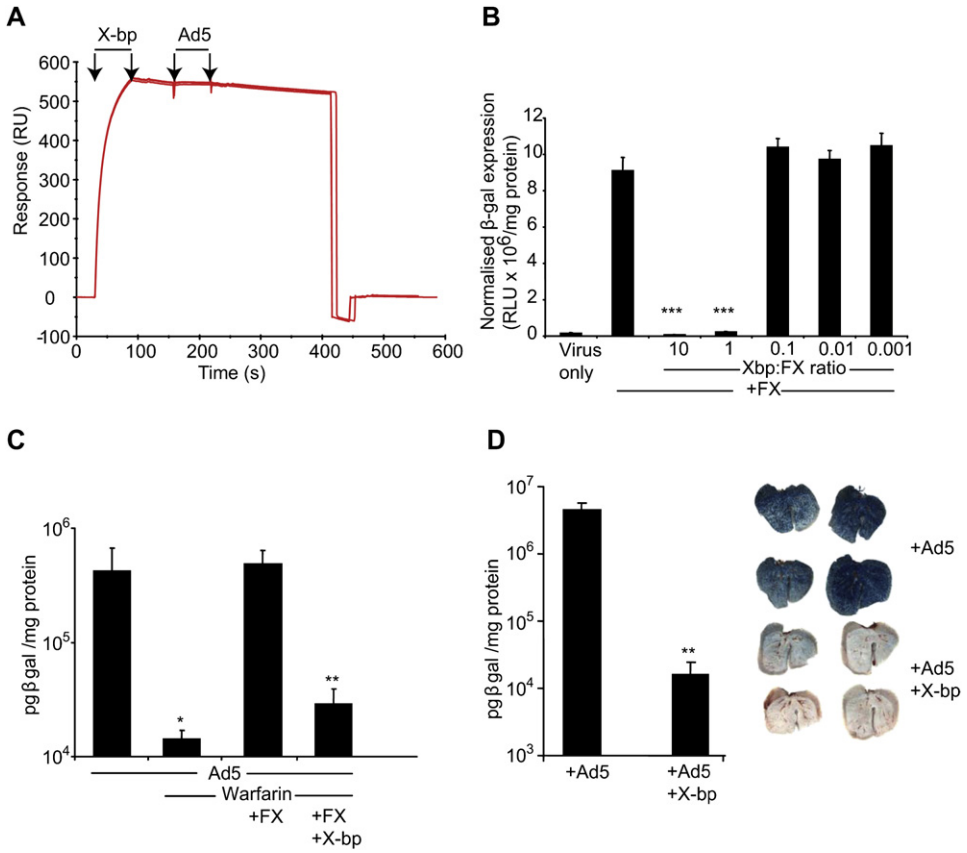

Figure 6. Pharmacological Blockade of Ad5 Binding to FX by Snake Venom Protein X-bp Blocks Liver Transduction In Vivo

(A) Subtracted SPR sensorgram (FX-FXI) shows X-bp binding with high affinity (increase in RU following X-bp injection) and ablates subsequent FX-Ad5 binding (no change in RU following Ad5 injection). Arrows indicate the start and end of reagent injection.

(B) HepG2 cells were exposed to AdKO1 in the presence of FX alone or FX preincubated with X-bp at different FX:X-bp molar ratios (as shown). ***$p < 0.0001$ versus no X-bp. Error bars represent SEM.

(C) MF-1 mice were pretreated with control peanut oil or warfarin and injected with 4×10^{11} VP/mouse Ad5 with or without preinjection of FX alone or preincubated with three-fold molar excess of X-bp. *$p = 0.006$; **$p = 0.0002$. Error bars represent SEM.

(D) MF-1 mice (nonwarfarinized) were injected with X-bp 30 min prior to Ad5 injection. Forty-eight hours later liver gene transfer was quantified by ELISA (bar graph) and visualized by staining for β-galactosidase (pictures). (**$p = 0.0002$). Error bars represent SEM.

application. The hexon protein is highly conserved between different serotypes (70%–80% sequence identity), but in the HVRs there are distinct amino acid sequence profiles. Phylogenetic analysis of the amino acid sequences of the HVRs identified two distinct clades corresponding to the D subgroup and the A, B, and C subgroups (Figure 7A) (Madisch et al., 2005). The observed difference in amino acid sequences in the HVRs most probably reflects the early divergence of subgroup D from A, B, and C. We tested the ability of diverse human Ad serotypes to bind FX by SPR (Figures 7A and 7B). Three phenotypes were detected—adenoviruses that bind strongly, indicated by ++ or +++ (e.g., Ad5, Ad2, Ad50, Ad16); adenoviruses that show weak FX binding, indicated by + (e.g., Ad35, Ad3); and adenoviruses that do not bind FX at all, indicated in blue (e.g., Ad48, Ad26) (Figures 7A and 7B). Viruses that do not bind FX all belong to the D subgroup (Figure 7A). We next assessed whether binding to FX correlated with FX sensitivity in cell binding and transduction in vitro and in vivo, focusing on Ad35 (weak binding) and Ad26 (no binding), vectors that are in clinical development, and comparing this to Ad5 (strong binding). Kinetic analysis by SPR for FX binding to Ad35 and Ad26 revealed for Ad35 a ka of 1.1×10^5 (1/Ms) and a kd of 5.7×10^{-3} (1/s), giving an overall K_D of 5.2×10^{-8}M (Figure S8) and for Ad26 no detectable binding even at 50 μg/ml FX (data not shown). The K_D for Ad35 is, as expected, significantly weaker than the Ad5-FX interaction. In vitro, Ad binding to and transduction of HepG2 cells was FX sensitive for Ad5 but not for Ad35 and Ad26 (Figure 7C). For Ad35, injection into CD46 transgenic mice in either the presence or absence of X-bp preinjection showed lung targeting (Figure 7D). For Ad26, intravascular administration into mice revealed a complete lack of liver transduction, either with or without preinjection of X-bp (Figure 7D). In vivo analysis of Ad48, a second non-FX binding serotype, also showed a lack of hepatic tropism (Figure 7D). Taken together with the observations on Ad26, this indicates that vectors derived from adenoviruses that show weak or no binding to FX are not influenced by the FX pathway in vivo. This has important implications for vector usage and engineering strategies for gene therapy applications.

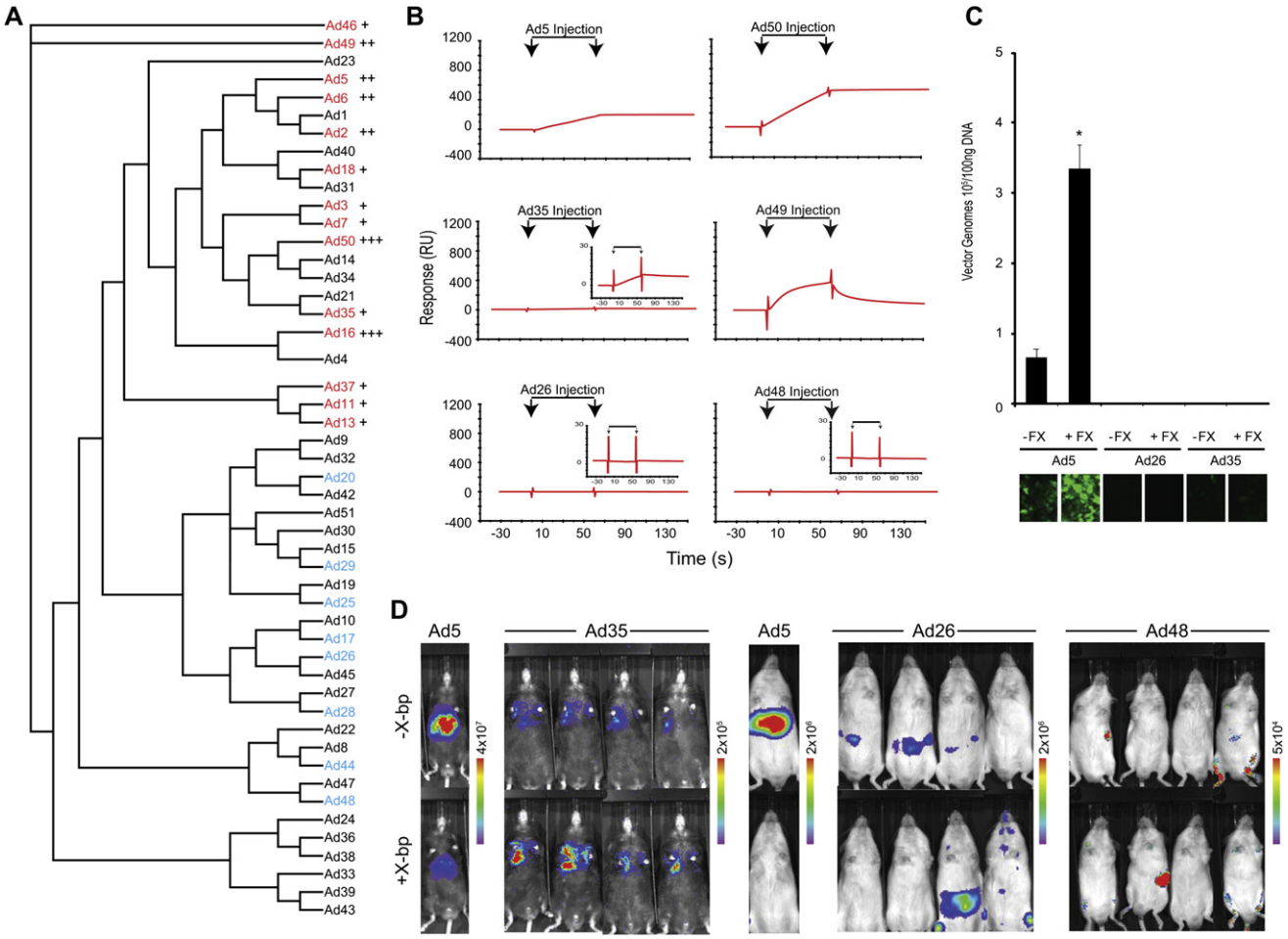

Figure 7. FX Binding to Alternate Human Adenovirus Serotypes

(A) Phylogenetic tree based on alignment of hexon HVR amino acid sequences by ClustalW and visualized by Treeview (http://taxonomy.zoology.gla.ac.uk/rod/treeview.html) showing FX binders (red) and nonbinders (blue) and strength of FX binding determined by SPR is indicated. Ad viruses not tested by SPR are shown in black.

(B) Representative SPR sensograms depict human adenovirus serotypes that show strong (++ or +++), weak (+), or no binding to FX. Insets show expanded *y* axis to show weak (Ad35) or not detectable binding (Ad26 and Ad48). Arrows indicate the start and end of injection.

(C) HepG2 cells were exposed to each adenovirus in the presence or absence of physiological FX. DNA was extracted and cell-bound adenovirus quantified. Error bars represent SEM (*$p < 0.05$ versus absence of FX). Images show transgene (eGFP) expression following exposure for 3 hr at 37°C in the presence/absence of FX.

(D) 5×10^{10} VP/mouse of Ad was injected either with or without 4.8 mg/kg X-bp in CD46 transgenic mice (Oldstone et al., 1999) for Ad5 and Ad35 or MF-1 mice for Ad5, Ad26, or Ad48. At 48 hr post-infection, mice were subject to whole-body bioluminescence quantitation.

DISCUSSION

We reveal an unexpected role for the Ad5 hexon protein for defining virus infectivity in vivo. The complex of Ad5 with FX, mediated through a molecular interaction between the FX Gla domain and the hexon HVRs, is the major pathway leading to in vivo delivery of adenovirus to hepatocytes from the bloodstream. This is supported by the over 150-fold reduction in liver transduction mediated by Ad5 in mice preinjected with X-bp, a snake venom-derived protein that blocks the molecular interaction of FX Gla and Ad5 hexon. Moreover, the chimeric Ad5 vector Ad5HVR48, which has only the HVRs of Ad48 swapped into the Ad5 hexon, displays abolished FX binding activity by SPR and in vitro assays as well as a substantial reduction in liver gene transfer. It is important to remark that all other capsid components in Ad5HVR48 are Ad5. The Ad5 fiber has no function in FX binding as swapping Ad5 hexon HVRs for those from the nonbinding Ad48 abolishes FX binding capacity. This pathway has fundamental implications for adenovirus biology and vector design for human gene therapy. Moreover, the role of the Ad hexon protein in cellular infectivity provides important information that may lead to the more effective development of safer gene therapies.

Previously, we and others have reported that liver transduction by CAR binding and CAR binding-mutated Ad5 vectors are equal (reviewed in Nicklin et al., 2005; Waddington et al., 2007). Clearly, fiber modifications have been shown to impact liver transduction, including Ad5 vectors pseudotyped with

alternative fibers and Ad5 vectors devoid of the putative heparan sulfate proteoglycan binding site in the fiber shaft (Koizumi et al., 2006; Smith et al., 2003; reviewed in Nicklin et al., 2005). However, mutation at this site may confer fiber rigidity since vectors possessing this mutation maintain the ability to bind cells but are not able to mediate transduction (Bayo-Puxan et al., 2006; Kritz et al., 2007). The lack of influence on liver transduction following mutation of the fiber and/or penton proteins (Nicol et al., 2004; Smith et al., 2003; Martin et al., 2003) suggests that these mutations have not identified the natural mechanism for Ad5 localization to hepatocytes following intravascular delivery. This is supported by the findings in our study as either pharmacological intervention or mutation of the Ad5 hexon protein block Ad5-FX interaction and liver transduction by Ad5 in vivo. Importantly, Ad5HVR48 is still able to mediate transduction at a comparable level to Ad5 following direct intramuscular injection, thus showing that this virus still retains the ability to interact with its other receptors in the appropriate in vivo setting. Together these findings support the assertion that interaction between the Ad5 hexon and FX is the major pathway that the virus utilizes to achieve localization to hepatocytes via the bloodstream. The roles of other capsid proteins, including the fiber and penton, in the entire liver transduction process relating to the FX-mediated pathway will be important to ascertain. Transduction is a complex series of mechanisms including cell attachment, internalization, and nuclear trafficking, and our modeling suggested projection of FX from the virion surface, thus potentially sterically influencing fiber-mediated interactions. Importantly, liver transduction is often a serious concern following local application of adenovirus in vivo (Hiltunen et al., 2000), hence simultaneous administration of an FX-Ad5 blocking agent may prevent such occurrence, thus improving safety.

Blocking the hexon-FX interaction could be achieved by HVR exchange as evidenced for Ad48 or by selective mutagenesis, although careful analysis of full serotype tropism would be required, ideally focusing on serotypes that offer lower sero-prevalence with respect to pre-existing antibodies in the human population (Roberts et al., 2006). This would create adenoviruses with both lower sero-prevalence in human populations and lacking FX binding. Alternatively, mutagenesis strategies for Ad5 hexon, focusing on key interacting locales in HVRs to ablate hexon-Ad5 interactions, will result in Ad5 mutants devoid of FX binding.

This study has implications for vector design using pseudotyping strategies involving swapping of alternate (non-Ad5) fibers onto the Ad5 capsid. Fibers derived from subgroup B Ads that bind CD46 are of particular interest, as they mediate enhanced Ad uptake into CD46-positive tissues, including tumors (Gaggar et al., 2003; Sakurai et al., 2006; Tuve et al., 2006). Since we show that Ad35 only weakly interacts with FX, it can be envisaged that development of full serotype Ad35 vectors may be more preferential than using a fiber-pseudotyping strategy alone since the Ad5 hexon will still bind FX within the context of a pseudotyped virus. This is exemplified by our recent analysis of adenoviruses pseudotyped with fibers from subgroup D, all of which showed direct binding to FX by SPR (in comparison to the divergent data on the full subgroup D viruses presented here), resulting in enhanced FX-mediated cell-surface binding and transduction (Parker et al., 2007). Furthermore, in vivo targeting of Ad5/47 (a virus pseudotyped with the fiber from the subgroup D virus Ad47) to the liver was sensitive to warfarin treatment, suggesting that the binding of FX to Ad5 hexon leads to efficient liver targeting and is dominant over any fiber effects (Waddington et al., 2007).

Taken together, this study identifies an unexpected function of adenovirus hexon in mediating in vivo liver gene transfer by Ad5 through recruitment of host FX to the hexon HVR and cell binding of the resulting complex through the FX serine protease. Moreover, this is an effect applicable to a number of alternate human serotypes and has implications for adenovirus vector development and safety for application to human gene therapy.

EXPERIMENTAL PROCEDURES

Materials

Purified blood coagulation factors (FX, FX-GD, protein C, and FXI) were purchased from Haematologic Technologies Inc (Essex Junction, VT). Recombinant (r) FIX (BeneFIX) was from Wyeth (Philadelphia, PA, USA). rFVII was sourced as described (Parker et al., 2006). rFX EGF2-SP was a kind gift of Daniel Johnson (Cambridge, UK). FX-GD was prepared by chymotrypsin digest of full-length FX (purchased from Haematologic Technologies Inc). The FX-GD was further purified by removal of uncleaved full-length FX using affinity chromatography with a monoclonal antibody to γ-carboxy glutamic acid residues (American Diagnostica, Stamford, CT, USA). rNAPc2 was a kind gift of Dr G. Vlasuk (Corvas International, San Diego, CA, USA). Antibodies were sourced as follows: HX-1 (Sigma, Poole, UK); monoclonal antibody 3570 against γ-carboxyglutamic acid residues (American Diagnostica). Ad5 hexon was purified from Ad5-infected cells according to the method of Rux et al. (1999). Adenoviruses were propagated in either PER.C6 cells (Vogels et al., 2003) or in 293 cells (Parker et al., 2006). FX levels were determined using a standard sandwich ELISA Asserachrom X:AG kit (Diagnostica Stago Inc., Parsipanny, NJ, USA). Plasma samples (1:9 ratio of blood: 3.8% sodium citrate anticoagulant) were loaded in duplicate at both 1/50 and 1/200 dilutions. The ELISA recognized both full-length FX and FX-GD with similar efficiency.

Surface Plasmon Resonance Analysis

SPR was performed using a Biacore T100 and a Biacore X (Biacore, Stevenage, UK) (Parker et al., 2006). Coagulation factors were covalently immobilized onto flowcells of CM5 biosensor chips by amine coupling according to the manufacturer's instructions. Virus in 10 mM HEPES (pH 7.4). 150 mM NaCl, 5 mM $CaCl_2$, 0.005% Tween 20 was passed over the chip at 30 μl/min. Sensorchips were regenerated between virus application by injection of 10 mM HEPES (pH 7.4), 150 mM NaCl, 3 mM EDTA, 0.005% Tween 20. FXa and EGF2-serine protease FXa were biotinylated with biotin-FPRCK (Haematologic Technologies Inc) at 25°C overnight and then dialyzed. Ad5 was biotinylated using the EZ-link sulfo-NHS-LC-biotinylation kit (Pierce, Rockford, IL, USA) according to the manufacturer's instructions. The biotinylated products were coupled to streptavidin coated sensorchips (SA; Biacore) according to the manufacturer's instructions. Rmax was calculated from the immobilized Ad5 (500 RU) using the formula: $Rmax = Mw_{FX} / Mw_{Ad5} \times R_l \times S$ where $s = 1$. To assess binding of Ad serotypes human (h) coagulation FXI and FX were covalently immobilized onto flowcells of a CM5 biosensor chip by amine coupling (hFXI, 8496 RU; hFX, 6460 RU). Ad serotypes (100–0.79 × 10^{10} vp/ml, 8 two-fold serial dilutions were analyzed in duplicate) were passed over the chip at 30 μl/min.

Kinetic Affinites of FX Inhibitors for Human and Mouse FX Determined by SPR

Human (h) coagulation FXI (731 RU), FX (584 RU), mouse (m) FX (548 RU), and purified Ad5 hexon (521 RU) were covalently immobilized onto flowcells of a CM5 biosensor chip by amine coupling. X-bp, rNapc2, and Ixolaris (10–0.078 μg/ml, 8 two-fold serial dilutions were analyzed in duplicate) or

coagulation factors (50–0.78 μg/ml, 7 two-fold serial dilutions analyzed in triplicate) were passed over the chip at 30 μl/min in 10 mM HEPES (pH 7.4), 150 mM NaCl, 5 mM $CaCl_2$, 0.005% Tween 20. Sensorchips were regenerated by injection of glycine pH 2 for the inhibitors and 10 mM HEPES (pH 7.4), 150 mM NaCl, 3 mM EDTA, 0.005% Tween 20 for coagulation factors. Kinetic analysis was performed using Biacore T100 evaluation software and fitted using a heterogeneous ligand model.

In Vitro Experiments

Human HepG2 cells were cultured in Dulbecco's Modified Eagle's Medium (DMEM, Biowhittaker), supplemented with 2 mM L-glutamine (Invitrogen, Paisley, UK) and 10% fetal calf serum (FCSPAA Laboratories, Yeovil, UK). SKOV-3 and MDA-MB-435 cells were maintained in RPMI 1640 media (Invitrogen) with 5% serum. For transgene expression, 2×10^4 cells/well were plated into 96-well plates and transferred to serum-free media containing 8 μg/ml FX (1 IU/ml; Cambridge Biosciences, Cambridge, UK). Virus was added at 1000 VP/cell for 3 hr at 37°C. Cells were maintained at 37°C until harvesting at 72 hr. In experiments with NAPc2 and Ixolaris, FX was preincubated for 30 min. X-bp and FX (1 IU/ml) were mixed at varying molar ratios (10–0.001) for 30 min. Expression of β-galactosidase was quantified using Tropix Galacto-Light Plus (Applied Biosystems, Foster City, CA, USA) using a Wallac VICTOR2 (PerkinElmer Life and Analytical Sciences, Boston, MA, USA) and recombinant β-galactosidase as standard. Protein concentrations were quantified by bicinchoninic acid assay (Perbio Science, Cramlington, UK). All data are expressed as relative light units (RLU) per milligram of protein. Cells were imaged using an Olympus BX40 microscope. Cell binding experiments were performed in 24-well plates and in serum free media ± FX at 4°C for 1 hr using 1000 VP/cell (unless otherwise stated). Viral and total genomic DNA were isolated using a QIAamp DNA mini kit (QIAGEN, Crawley, UK), quantified by NanoDrop (ND-1000 spectrophotometer [Labtech International, Ringmer, UK]). One hundred nanograms of total DNA was subject to quantitative PCR analysis using an ABI prism 7900HT Sequence detection system (Applied Biosystems, Warrington, UK) using the *Power* SYBR Green PCR Master Mix as described (Parker et al., 2006). Total Ad genomes were calculated using the SDS 2.3 software and using a standard curve of 10^2–10^7 Ad particles.

Electron Cryomicroscopy

Ad5 was incubated in the presence of an approximate three-fold excess of FX overnight at 4°C. Complexed and noncomplexed virus was prepared for electron cryomicroscopy as previously described (Adrian et al., 1984). Briefly, 5 μl of virus was loaded onto a freshly glow-discharged Quantifoil holey carbon support film (R2/2 Quantifoil Micro Tools GmbH, Jena, Germany), blotted, and plunged into a bath of liquid nitrogen cooled ethane slush. Vitrified specimens were imaged at low temperature in a JEOL 1200 EXII transmission electron microscope equipped with an Oxford instruments CT3500 cryo-transfer stage. Low-dose focal pair images were recorded at 30,000 × magnification on Kodak SO163 film.

Three-Dimensional Image Reconstruction

Twenty and twenty-one focal pairs of micrographs were selected on the basis of optimal ice-thickness for unlabeled and labeled virus, respectively. These were digitized on a Nikon Super Coolscan 9000ED CCD scanner at 4000 dpi resolution, corresponding to 2.18 Å/pixel in the specimen. Scanned micrographs were then converted to PIF (Purdue image format) and binned by a factor of three using the BSOFT image-processing package (Heymann, 2001), giving a final raster step size of 6.54 Å/pixel. X3D was used to select and cut out individual particles; these were then processed to correct imaging artifacts by determining the defocus of each micrograph and inverting successive oscillations of the contrast-transfer function using the CTFMIX program. Subsequently, full CTF correction was applied, merging defocus paired particle images (Conway and Steven, 1999). To calculate an initial reconstruction for unlabeled Ad5, a common-lines approach was taken using a modified version of the MRC icosahedral reconstruction suite of programs (Crowther et al., 1970; Fuller et al., 1996). Following calculation of a preliminary reconstruction, a modified version of the polar Fourier transform method (PFT2) was used to determine and refine origins and orientations for each particle in both complexed and noncomplexed data sets (Baker and Cheng, 1996; Bubeck et al., 2005). Resolution assessment for the final reconstructions was performed by dividing each data set into equal halves. These were used to calculate two independent reconstructions. A number of measures of agreement were calculated for the two density maps, including the Fourier shell correlation and spectral signal to noise ratio, using the BSOFT program bresolve. Reconstructions were visualized using UCSF Chimera (Pettersen et al., 2004). The Ad5-FX reconstruction is deposited in the EM database with accession code EMD-1464.

In Vivo Methods

MF-1 outbred mice (Harlan, UK) or CD46 transgenic mice (Oldstone et al., 1999) 25–30 g were used for all experiments. In some experiments, 5 mg/kg warfarin suspended in peanut oil was injected subcutaneously 3 and 1 days prior to Ad5 administration to ablate circulating levels of functional vitamin K-dependent coagulation factors as described (Parker et al., 2006; Waddington et al., 2007). For NAPc2 and Ixolaris experiments, 400 μg/kg of NAPc2 or 0.78 mg/kg Ixolaris were pre-mixed with FX 30 min prior to intravenous injection of both. For X-bp studies we injected 4.8 mg/kg X-bp intravascularly in warfarin-treated mice or into normal (nonwarfarinized) mice 30 min before injection of adenovirus. For Ad5 versus Ad5HVR48 intravascular injection experiments, mice received 200 μl intravenous clodronate liposomes (Van Rooijen and Sanders, 1994) 24 hr before adenovirus. For intramuscular injections 1×10^{10} VP/mouse was injected into the tibialis anterior. Mice were subject to whole-body bioluminescence quantitation (IVIS-50, Xenogen, USA) or were sacrificed for analysis of tissue expression of β-galactosidase as described (Waddington et al., 2007).

Statistical Analysis

In vitro experiments were performed in triplicate on at least three independent occasions. In vivo experiments were performed with at least four animals per group. Where necessary, data were normalized by logarithmic transformation. Analysis was either by unpaired Student's t test or for multiple comparisons, analysis of variance and Tukey's pairwise comparison using MINITAB software.

Supplemental Data

Supplemental Data include one table and eight figures and can be found with this article online at http://www.cell.com/cgi/content/full/132/3/397/DC1/.

ACKNOWLEDGMENTS

We thank Erguang Li for the plasmids to make Ad5-21R and Ad5-7.5R, Linda Klavinskis for CD46 transgenic mice, and Dan Johnson for the EGF2-SP FX. We thank Professor Charles Coutelle for helpful discussions. We thank Nicola Britton and Gregor Aitchison for technical support and Lennart Holterman for virus production. Gary Childs and staff provided valuable technical support for in vivo studies. Professor Gadi Frankel and Siouxsie Wiles (Imperial College London) provided training and access to the Xenogen equipment. This work was supported by the European Commission, the Biotechnology and Biophysical Research Council, and British Heart Foundation. Haemostasis and Thrombosis are supported by the Medical Research Council. A.L.P. is funded by a Personal Research Fellowship from the Caledonian Research Foundation. S.W. is a recipient of the Philip Gray Fellowship, Katharine Dormandy Trust.

Received: October 19, 2007
Revised: December 10, 2007
Accepted: January 15, 2008
Published: February 7, 2008

REFERENCES

Abbink, P., Lemckert, A.A.C., Ewald, B.A., Lynch, D.M., Denholtz, M., Smits, S., Holterman, L., Damen, I., Vogels, R., Thorner, A.R., et al. (2007). Comparative seroprevalence and immunogenicity of six rare serotype recombinant adenovirus vaccine vectors from Subgroups B and D. J. Virol. *81*, 4654–4663.

Adrian, M., Dubochet, J., Lepault, J., and McDowall, A. (1984). Cryo-electron microscopy of viruses. Nature *308*, 32–36.

Alemany, R., and Curiel, D.T. (2001). CAR-binding ablation does not change biodistribution and toxicity of adenoviral vectors. Gene Ther. *8*, 1347–1353.

Athappilly, F., Murali, R., Rux, J., Cai, Z., and Burnett, R. (1995). The refined crystal structure of hexon, the major coat protein of adenovirus type 2, at 29 A resolution. J. Mol. Biol. *242*, 430–455.

Atoda, H., Ishikawa, M., Mizuno, H., and Morita, T. (1998). Coagulation factor X-binding protein from *Deinagkistrodon acutus* venom is a gla domain-binding protein. Biochemistry *37*, 17361–17370.

Baker, T.S., and Cheng, R. (1996). A model-based approach for determining orientations of biological macromolecules imaged by cryoelectron microscopy. J. Struct. Biol. *116*, 120–130.

Bayo-Puxan, N., Cascallo, M., Gros, A., Huch, M., Fillat, C., and Alemany, R. (2006). Role of the putative heparan sulfate glycosaminoglycan-binding site of the adenovirus type 5 fiber shaft on liver detargeting and knob-mediated retargeting. J. Gen. Virol. *87*, 2487–2495.

Bergelson, J.M., Cunningham, J.A., Droguett, G., Kurt-Jones, E.A., Krithivas, A., Hong, J.S., Horwitz, M.S., Crowell, R.L., and Finberg, R.W. (1997). Isolation of a common receptor for coxsackie B viruses and adenoviruses 2 and 5. Science *275*, 1320–1323.

Bubeck, D., Filman, D., Cheng, N., Steven, A., Hogle, J., and Belnap, D. (2005). The structure of the poliovirus 135S cell entry intermediate at 10-angstrom resolution reveals the location of an externalized polypeptide that binds to membranes. J. Virol. *79*, 7745–7755.

Conway, J., and Steven, A. (1999). Methods for reconstructing density maps of "single" particles from cryoelectron micrographs to subnanometer resolution. J. Struct. Biol. *128*, 106–118.

Crowther, R., Amos, L., Finch, J., De Rosier, D., and Klug, A. (1970). Three dimensional reconstructions of spherical viruses by fourier synthesis from electron micrographs. Nature *226*, 421–425.

Fuller, S., Butcher, S., Cheng, R., and Baker, T.S. (1996). Three-dimensional reconstruction of icosahedral particles–the uncommon line. J. Struct. Biol. *116*, 48–55.

Gaggar, A., Shayakhmetov, D.M., and Lieber, A. (2003). CD46 is a cellular receptor for group B adenoviruses. Nat. Med. *9*, 1408–1412.

Heymann, J. (2001). Bsoft: image and molecular processing in electron microscopy. J. Struct. Biol. *133*, 156–169.

Hiltunen, M.O., Turunen, M.P., Turunen, A.-M., Rissanen, T.T., Laitinen, M., Kosma, V.-M., and Yla-Herttuala, S. (2000). Biodistribution of adenoviral vector to nontarget tissues after local *in vivo* gene transfer to arterial wall using intravascular and periadventitial gene delivery methods. FASEB J. *14*, 2230–2236.

Huard, J., Lochmuller, H., Ascadi, G., Jani, A., Massie, B., and Karpati, G. (1995). The route of administration is a major determinant of the transduction efficiency of rat tissues by adenoviral recombinants. Gene Ther. *107*, 107–115.

Kawabata, K., Sakurai, F., Koizumi, N., Hayakawa, T., and Mizuguchi, H. (2006). Adenovirus vector-mediated gene transfer into stem cells. Mol. Pharm. *3*, 95–103.

Koizumi, N., Kawabata, K., Sakurai, F., Watanabe, Y., Hayakawa, T., and Mizuguchi, H. (2006). Modified adenoviral vectors ablated for coxsackie-adenovirus, α_v integrin, and heparan sulphate binding reduce in vivo tissue transduction and toxicity. Hum. Gene Ther. *17*, 264–279.

Kritz, A., Nicol, C., Dishart, K., Nelson, R., Holbeck, S., Von Seggern, D., Work, L., McVey, J., Nicklin, S., and Baker, A. (2007). Adenovirus 5 fibers mutated at the KKTK putative HSPG binding site show restricted retargeting capacity when engineered with targeting peptides in the HI loop. Mol. Ther. *15*, 741–749.

Lecollinet, S., Gavard, F., Havenga, M.J.E., Spiller, O.B., Lemckert, A., Goudsmit, J., Eloit, M., and Richardson, J. (2006). Improved gene delivery to intestinal mucosa by adenoviral vectors bearing subgroup B and D fibers. J. Virol. *80*, 2747–2759.

Li, J., Lad, S., Yang, G., Luo, Y., Iacobelli-Martinez, M., Primus, F.J., Reisfeld, R.A., and Li, E. (2006). Adenovirus fiber shaft contains a trimerization element that supports peptide fusion for targeted gene delivery. J. Virol. *80*, 12324–12331.

Madisch, I., Harste, G., Pommer, H., and Heim, A. (2005). Phylogenetic analysis of the main neutralization and hemagglutination determinants of all human adenovirus prototypes as a basis for molecular classification and taxonomy. J. Virol. *79*, 15265–15276.

Martin, K., Brie, A., Sauliner, P., Perricaudet, M., Yep, P., and Vigne, E. (2003). Simultaneous CAR- and α_v integrin-binding ablation fails to reduce Ad5 liver tropism. Mol. Ther. *8*, 485–494.

Monteiro, R., Rezaie, A., Ribeiro, J., and Francishetti, I. (2005). Ixolaris: a factor Xa heparin-binding exosite inhibitor. Biochem. J. *387*, 871–877.

Murakami, M.T., Rios-Steiner, J., Weaver, S.E., Tulinsky, A., Geiger, J.H., and Arni, R.K. (2007). Intermolecular interactions and characterization of the novel factor Xa exosite involved in macromolecular recognition and inhibition: Crystal structure of human Gla-domainless factor Xa complexed with the anticoagulant protein NAPc2 from the hematophagous nematode *Ancylostoma caninum*. J. Mol. Biol. *366*, 602–610.

Nicklin, S., Wu, E., Nemerow, G., and Baker, A. (2005). The influence of adenovirus fiber structure and function on vector development for gene therapy. Mol. Ther. *12*, 384–393.

Nicol, C.G., Graham, D., Miller, W.H., White, S.J., Smith, T.A., Nicklin, S.A., Stevenson, S.C., and Baker, A.H. (2004). Effect of adenovirus serotype 5 fiber and penton modifications on in vivo tropism in rats. Mol. Ther. *10*, 344–354.

Oldstone, M., Lewicki, H., Thomas, D., Tishon, A., Dales, S., Patterson, J., Manchester, M., Homann, D., Naniche, D., and Holz, A. (1999). Measles virus infection in a trasgenic model: virus-induced immunosuppression and central nervous system disease. Cell *98*, 629–640.

Parker, A.L., Waddington, S.N., Nicol, C.G., Shayakhmetov, D.M., Buckley, S.M., Denby, L., Kemball-Cook, G., Ni, S., Lieber, A., McVey, J.H., et al. (2006). Multiple vitamin K-dependent coagulation zymogens promote adenovirus-mediated gene delivery to hepatocytes. Blood *108*, 2554–2561.

Parker, A.L., McVey, J.H., Doctor, J.H., Lopez-Franco, O., Waddington, S.N., Havenga, M.J.E., Nicklin, S.A., and Baker, A.H. (2007). Influence of coagulation factor zymogens on the infectivity of adenoviruses pseudotyped with fibers from subgroup D. J. Virol. *81*, 3627–3631.

Pettersen, E., Goddard, T., Huang, C., Couch, G., Greenblatt, D., Meng, E., and Ferrin, T. (2004). UCSF chimera–a visualization system for exploratory research and analysis. J. Comput. Chem. *25*, 1605–1612.

Pichla-Gollon, S.L., Drinker, M., Zhou, X., Xue, F., Rux, J.J., Gao, G.-P., Wilson, J.M., Ertl, H.C., Burnett, R.M., and Bergelson, J.M. (2007). Structure-based identification of a major neutralizing site in an adenovirus hexon. J. Virol. *81*, 1680–1689.

Raper, S.E., Chirmule, N., Lee, F.S., Wivel, N.A., Bagg, A., Gao, G.-P., Wilson, J.M., and Batshaw, M.L. (2003). Fatal systemic inflammatory response syndrome in a ornithine transcarbamylase deficient patient following adenoviral gene transfer. Mol. Genet. Metab. *80*, 148–158.

Rezaie, A.R. (2000). Identification of basic residues in the heparin-binding exosite of factor Xa critical for heparin and factor Va binding. J. Biol. Chem. *275*, 3320–3327.

Roberts, D., Nanda, A., Havenga, M., Abbink, P., Lynch, D., Ewald, B., Liu, J., Thorner, A., Swanson, P., Gorgone, D., et al. (2006). Hexon-chimaeric adenovirus serotype 5 vectors circumvent pre-existing anti-vector immunity. Nature *441*, 239–243.

Roberts, M., White, J., Grutter, M., and Burnett, R. (1986). Three-dimensional structure of the adenovirus major coat protein hexon. Science *232*, 1148–1151.

Rux, J., and Burnett, R. (2000). Type-specific epitope locations revealed by X-ray crystallographic study of adenovirus type 5 hexon. Mol. Ther. *1*, 18–30.

Rux, J.J., Pascolini, D., and Burnett, R.M. (1999). Large-scale purification and crystallization of adenovirus hexon. In Methods in Molecular Medicine, Vol 21:

Adenovirus Methods and Protocols, W.S.M. Wold, ed. (Totowa NJ: Humana Press Inc.), pp. 259–275.

Sakurai, F., Kawabata, K., Koizumi, N., Inoue, N., Okabe, M., Yamaguchi, T., Hayakawa, T., and Mizuguchi, H. (2006). Adenovirus serotype 35 vector-mediated transduction into human CD46-transgenic mice. Gene Ther. *13*, 1118–1126.

San Martin, C., and Burnett, R. (2003). Structural studies on adenoviruses. Curr. Top. Microbiol. Immunol. *272*, 57–94.

Segerman, A., Atkinson, J.P., Marttila, M., Dennerquist, V., Wadell, G., and Arnberg, N. (2003). Adenovirus type 11 uses CD46 as a cellular receptor. J. Virol. *77*, 9183–9191.

Shayakhmetov, D.M., Papayannopoulou, T., Stamatoyannopoulos, G., and Lieber, A. (2000). Efficient gene transfer into human CD34+ cells by a retargeted adenovirus vector. J. Virol. *74*, 2567–2583.

Shayakhmetov, D., Li, Z., Ni, S., and Lieber, A. (2002). Targeting of adenovirus vectors to tumor cells does not enable efficient transduction of breast cancer metastases. Cancer Res. *62*, 1063–1068.

Shayakhmetov, D., Gaggar, A., Ni, S., Li, Z.-Y., and Lieber, A. (2005). Adenovirus binding to blood factors results in liver cell infection and hepatotoxicity. J. Virol. *79*, 7478–7491.

Schenk-Braat, E.A.M., van Mierlo, M.M.K.B., Wagemaker, G., Bangma, C.H., and Kaptein, L.C.M. (2007). An inventory of shedding data from clinical gene therapy trials. J. Gene Med. *9*, 910–921.

Smith, T.A.G., Idamakanti, N., Marshall-Neff, J., Rollence, M.L., Wright, P., Kaloss, M., King, L., Mech, C., Dinges, L., Iverson, W.O., et al. (2003). Receptor interactions involved in adenoviral-mediated gene delivery after systemic administration in non-human primates. Hum. Gene Ther. *14*, 1595–1604.

Sumida, S.M., Truitt, D.M., Lemckert, A.A.C., Vogels, R., Custers, J.H.H.V., Addo, M.M., Lockman, S., Peter, T., Peyerl, F.W., Kishko, M.G., et al. (2005). Neutralizing antibodies to adenovirus serotype 5 vaccine vectors are directed primarily against the adenovirus hexon protein. J. Immunol. *174*, 7179–7185.

Tomko, R.P., Xu, R., and Philipson, L. (1997). HCAR and MCAR: The human and mouse cellular receptors for subgroup C adenoviruses and group B coxsackieviruses. Proc. Natl. Acad. Sci. USA *94*, 3352–3356.

Tuve, S., Wang, H., Ware, C., Liu, Y., Gaggar, A., Bernt, K., Shayakhmetov, D., Li, Z., Strauss, R., Stone, D., and Lieber, A. (2006). A new group B adenovirus receptor is expressed at high levels on human stem and tumor cells. J. Virol. *80*, 12109–12120.

Van Rooijen, N., and Sanders, A. (1994). Liposome mediated depletion of macrophages: mechanism of action, preparation of liposomes and applications. J. Immunol. Methods *174*, 83–93.

Venkateswarlu, D., Perera, L., Darden, T., and Pedersen, L. (2002). Structure and dynamics of zymogen human blood coagulation factor X. Biophys. J. *82*, 1190–1206.

Vogels, R., Zuijeest, D., Rijnsoever, R.V., Hartkoorn, E., Damen, I., Bethune, M.-P.D., Kostense, S., Penders, G., Helmus, N., Koudstaal, W., et al. (2003). Replication-deficient human adenovirus type 35 vectors for gene transfer and vaccination: efficient human cell infection and bypass of preexisting adenovirus immunity. J. Virol. *77*, 8263–8271.

Von Seggern, D.J., Chiu, C.Y., Fleck, S.K., Stewart, P.L., and Nemerow, G.R. (1999). A helper-independent adenovirus vector with E1, E3 and fiber deleted: Structure and infectivity of fiberless particles. J. Virol. *73*, 1601–1608.

Waddington, S., Parker, A., Havenga, M., Nicklin, S., Buckley, S., McVey, J., and Baker, A. (2007). Targeting of adenovirus serotype 5 (Ad5) and 5/47 pseudotyped vectors *in vivo*: A fundamental involvement of coagulation factors and redundancy of CAR binding by Ad5. J. Virol. *81*, 9568–9571.

Wickham, T.J., Mathias, P., Cheresh, D.A., and Nemerow, G.R. (1993). Integrins $\alpha_v\beta_3$ and $\alpha_v\beta_5$ promote adenovirus internalization but not virus attachment. Cell *73*, 309–319.